Heliyon 10 (2024) e34657

Contents lists available at ScienceDirect

Heliyon

journal homepage: www.cell.com/heliyon

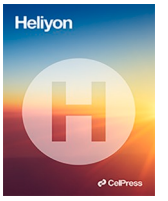

Research article

Application of South African heulandite (HEU) zeolite for the adsorption and removal of Pb^{2+} and Cd^{2+} ions from aqueous water solution: Experimental and computational study

Fred S. Wanyonyi [a], Francis Orata [a], Gershom K. Mutua [a], Michael O. Odey [b], Sizwe Zamisa [d], Sopuruchukwu E. Ogbodo [b,*], Francis Maingi [e], Anthony Pembere [c,**]

[a] Department of Pure and Applied Chemistry, Masinde Muliro University of Science and Technology, P.O Box 190, Kakamega, 50100, Kenya
[b] Computational and Bio-Simulation Research Group, University of Calabar, Calabar, Nigeria
[c] Department of Physical Sciences, Jaramogi Oginga Odinga University of Science and Technology, P.O Box 210, Bondo, 40601, Kenya
[d] School of Chemistry and Physics, University of Kwazulu-Natal, Westville Campus, Private Bag X 54001, Durban, 4001, South Africa
[e] Department of Science, Technology and Engineering, Kibabii University, PO Box 1699, Bungoma, 50200, Kenya

ARTICLE INFO

Keywords:
Adsorption
Pb^{2+}
Cd^{2+}
Heulandite zeolite
Isotherms
Molecular simulation

ABSTRACT

The capacity of South African Heulandite (HEU) zeolite to remove Pb^{2+} and Cd^{2+} ions from aqueous solution was investigated using batch experiments and molecular simulations studies. The effect of different factors on the adsorption of these ions onto the zeolite was investigated; contact time, initial metal ion concentration and the amount of HEU adsorbent. Molecular simulations was done using Monte Carlo and density functional theory. Experimental results obtained indicate that the maximum adsorption for the two ions occur at pH 5 and after 240 min of contact time. The percent removal based on contact time of Pb^{2+} and Cd^{2+} ions from water by the heulandite zeolite were 99.7 and 76.7 %, respectively. The adsorption of two metal ions onto the HEU zeolite follows the Langmuir adsorption isotherm. From the molecular simulation findings, the adsorption of Pb^{2+} ions onto the HEU window is equidistant from the two adjacent oxygen atoms within the HEU structure while the Cd^{2+} ion is adsorbed in the upper left side of the 8-ring HEU window. It was observed that the performance of the zeolite can significantly be improved by doping with germanium, aluminum, thallium indium, and sodium cations. These results indicate that the application of HEU zeolite as an adsorbent holds a great promise in heavy metal removal from aqueous solutions.

1. Introduction

Heavy metal pollution in the various environmental segments is of a global concern [1,2]. This is because heavy metals are toxic, non-biodegradable [3], and have a large dispersal capability and high rates of bioaccumulation in plants, animals and human [4,5]. Therefore, it is important to find ways of removing them from water [6–9]. Many wastewater treatment techniques aimed at the

* Corresponding author.
** Corresponding author.
E-mail addresses: ogbodosopuruchukwue@gmail.com (S.E. Ogbodo), apembere@jooust.ac.ke (A. Pembere).

https://doi.org/10.1016/j.heliyon.2024.e34657
Received 5 November 2023; Received in revised form 21 June 2024; Accepted 14 July 2024
Available online 15 July 2024

removal of numerous pollutants including heavy metals have been developed [10]. They include; chemical precipitation, electrochemical methods [11,12], ion exchange, membrane filtration, reverse osmosis, coagulation [13] and bio-sorption [14]. Nevertheless, most of these methods are ineffective, expensive, energy intensive and generate large amounts of toxic sludge [15,16]. Adsorption is one of the most common environmentally friendly technique use for the removal of pollutants from water [17–19]. In this respect, studies have focused on different types of adsorbents such as zeolites, activated carbon, clay and metal oxides. The use of natural materials as adsorbents has been the most commonly tested method owing to their cost effectiveness.

Zeolites are inorganic aluminosilicate solids with well-defined crystalline structures and micropore architecture [20]. They are classified as either natural or synthetic. The chemical composition of natural zeolitic materials vary depending on their geographical origin due different geochemical conditions [21]. Consequently, zeolites exhibit difference in chemical composition, structure, pore volume and surface area and cation exchange capacity [22]. Nevertheless, zeolites remain gorgeous adsorbents due to their impressive qualities, such as high chemical and thermal stability, large specific surface area, high affinity for heavy metal ions, prominent ion-exchange capacity, uniform pore sizes of molecular dimensions and recyclability [23,24]. Heulandite (HEU) is an important class of natural hydrated zeolites [25,26]. In general HEU zeolites have Si/Al ratio of less than 4 and they primarily have Ca^{2+} extra-framework cations [27]. The existing techniques for removing heavy metals from aqueous environments present notable challenges. For instance, electrocoagulation struggles with removing infinitely soluble particles, while precipitation methods often lack selectivity and are pH-sensitive, requiring meticulous control (Khandegar et al., 2013). These challenges underscore the necessity for more effective and selective removal methods. This research endeavors to bridge this gap by exploring the efficacy of doped HEU zeolite structures in removing Pb^{2+} and Cd^{2+} from water, aiming to provide insights into addressing the shortcomings of current removal techniques. Numerous studies have documented the ability of clinoptilolites from different sources in removing heavy metal ions from aqueous solutions [28]. For example; Kapanji used South African HEU zeolite to remove, Co^{2+}, Ni^{2+} Cu^{2+}, and Cr^{3+} ions from wastewater [29]. However, the study did not investigate the ability of HEU in removing Pb^{2+} and Cd^{2+}. Computational simulations have been employed to study the adsorption process of anions and cations from aqueous solutions [30]. It gives insights into the adsorption processes between the adsorbent and adsorbate at molecular level. Therefore, it complements and assist in interpretation of the batch experiment observations. For example, it provides information on the energy changes during adsorptions and the location where adsorption takes place [30,31].This study investigates the novelty of doped HEU zeolite structures by substituting silicon atoms with other elements. The efficacy of these doped HEU zeolites in removing Pb^{2+} and Cd^{2+} from aqueous solutions was assessed through batch experiments and molecular simulations, Prior studies on zeolites' adsorption capabilities have predominantly focused on different types of heavy metals or other contaminants, often overlooking the potential of doped zeolite structures for targeting specific heavy metal ions like Pb^{2+} and Cd^{2+}. Monte Carlo simulations computed the adsorption isotherms in the Grand Canonical ensemble (GCMC), which were used in evaluating the performance of the undoped and doped HEU. Therefore, this study provides valuable insights into the use of HEU zeolite as an efficacious adsorbent in removing Pb^{2+} and Cd^{2+} from water to alleviate water pollution. The unique contribution of this study lies in its exploration of naturally occurring sustainable adsorbent for removing Pb^{2+} and Cd^{2+} from aqueous solutions. This approach introduces a novel method to potentially address limitations in existing heavy metal removal techniques, offering a promising avenue for more effective water pollution mitigation strategies.

2. Experimental and computational methods

2.1. Materials

High purity Pb $(NO_3)_2$ (≥99.95 %) and Cd $(NO_3)_2$ (99.9 %), NaOH (≥98 %), HCl (37 %), NaCl (≥99 %) and solvents were supplied by Merck (Pty) Ltd through Kobian Kenya Ltd. The natural HEU zeolite was obtained from South Africa.

2.2. Characterization of HEU zeolite adsorbent

The HEU zeolite was ground and sieved using a 200-mesh sieve, then washed with deionized water and oven-dried overnight at 100 °C. No additional treatment was done prior to instrumental characterization and adsorption studies. Energy dispersive X-ray spectroscopy (EDX) (Shimadzu EDX-800HS), X-ray diffraction (XRD) (Rigaku Model-MiniFlex 600), and Fourier transform infrared spectroscopy (FTIR) (Nicolet 6700 FT-IR) techniques were used to characterize the HEU for its chemical composition, surface morphology and functional groups, respectively [32].

2.3. Batch adsorption experiments

The effect of reaction time, initial metal ion concentration and the amount of HEU zeolite on the adsorption of Pb^{2+} and Cd^{2+} onto HEU zeolite was investigated. Stock solution of Pb^{2+} (100 ppm) and Cd^{2+} (20 ppm) were prepared by dissolving $Pb(NO_3)_2$ and Cd $(NO_3)_2$ in deionized water. To determine the effect of contact time, the reaction time was varied from 0 to 240 min. To investigate the effect of initial concentration, the concentration of Pb^{2+} ion was varied from 5 to 30 ppm and that of Cd^{2+} from 1 to 3 ppm. Lastly, the effect of adsorbent dose was monitored by changing the amount of zeolite from 0.3 to 2 g. All the experiments were carried out in 250 mL erlenmeyer flasks at a constant temperature of 25 °C and agitated at 150 rpm using 50 mL of the metal ion solutions. After a predetermined time, the solutions were allowed to settle for 30 min, filtered off to determine the residual concentrations of the adsorbate at wavelength of 217 and 228.8 nm, using atomic absorption spectrophotometry (AAS) (Shimadzu AA-7000 Series). The equilibrium adsorption capacity and the percent removal of two metal ions was determined using equations (1) and (2).

Table 1
Chemical composition of the HEU zeolite.

Oxide	SiO_2	Al_2O_3	MgO	K_2O	CaO
Weight %	76.35	11.66	4.59	3.39	1.61

$$q_e = \frac{(C_i - C_f)V}{m} \tag{1}$$

$$R\% = \frac{(C_i - C_f)V}{C_i} \times 100 \tag{2}$$

Where; q_e- quantity of solute adsorbed per unit mass of adsorbent (mg/g), C_i - initial concentration of the metal ion (ppm), C_f - the final concentration the metal ion, m - the adsorbate mass (g), V- the volume of the metal ions solution (L) and R% - the metal ion removal percentage

The relationship between the amount of the adsorbate that was adsorbed and the residual concentration in the solution was then used to plot the adsorption isotherms using the obtained data. To determine the mechanism of adsorption of the two metal ions onto HEU zeolite, the data obtained was fitted into the Langmuir (equation (3)) and Freundlich (equation (4)) isotherms.

$$q_e = \frac{q_m K_l C_e}{1 + K_l C_e} \tag{3}$$

Where; q_e -adsorption capacity at equilibrium (mg/g), C_e-the concentration of adsorbate at equilibrium (ppm), K_L– the Langmuir constant (L/mg) and q_m -the monolayer adsorption capacity (mg/g) [33–35].

$$q_e = K_F C_e^{\frac{1}{n}} \tag{4}$$

where; q_e-the equilibrium adsorption capacity, K_F -the Freundlich constant, Ce-the concentration of heavy metal solution at equilibrium, n -the Freundlich exponent [36,37].

2.4. Computational modeling

Computational modeling plays a vital role in advancing our comprehension of adsorption mechanisms, especially in heavy metal removal. By simulating the molecular interactions between adsorbents and adsorbates, computational models offer a cost-efficient and time-effective approach to exploring various adsorption scenarios and predicting behavior under different conditions. This predictive capability proves invaluable in shaping experimental design and decision-making processes during the development of adsorption processes and materials (Sprenger et al., 2015). However, it's crucial to acknowledge the constraints of computational modeling in comprehending adsorption mechanisms. A notable limitation lies in the simplifications and assumptions inherent in computational models, which may not fully capture the intricacies of real-world systems. The accuracy of computational predictions heavily depends on input parameters like force fields and initial configurations, which can introduce uncertainties and errors into the outcomes. Additionally, computational modeling is restricted by computational resources and the level of theoretical approximation utilized. Complex systems or large-scale simulations may demand significant computational power and could be computationally intensive, imposing practical limitations on the extent and scale of simulations. Despite these challenges, computational modeling remains a potent tool for delving into adsorption mechanisms and guiding experimental endeavors in developing innovative technologies for heavy metal removal. Combining computational modeling with experimental approaches can synergistically enhance our understanding and facilitate more efficient and sustainable solutions to environmental pollution challenges (Zeigler et al., 2000).

The HEU zeolite structure was obtained from the Zeolite database [38]. Material Studio 17.0 software was used for the molecular simulations. We applied the first-principles DMol [3] method for the geometry optimizations of the heavy metals [39]. Natural bond orbital (NBO) population analyses were conducted using NBO 3.1 program fixed in the Gaussian 09 program [40]. The quantum theory of atoms-in-molecules (QTAIM) investigation was done using Multiwfn 3.7 software [41]. The effect of doping the HEU zeolite with different metal ions (germanium, aluminum, thallium, indium, and sodium) was also investigated in detail.

3. Results and discussion

3.1. Characterization of the HEU zeolite

Elemental data results obtained from the EDX analysis showed that SiO_2 is the most abundant compound in the HEU zeolite followed by Al_2O_3 (Table 1). The Si/Al ratio in the zeolite was 3.7. This affirmed that the zeolite used in this study is HEU zeolite since the ratio is less than 4[42]. Since the Si/Al ratio in the zeolite is less than 5, this zeolite can be described as low silica zeolite and therefore more acidic making it ideal for ion-exchange reactions [43,44]. In addition, the zeolite contained small amounts of K, Ca and Mg. However, there were no traces of lead and cadmium compounds in the zeolite.

The HEU zeolite was also analyzed using XRD and its characterization results are shown in Figs. 1 and 2. The structure of the zeolite

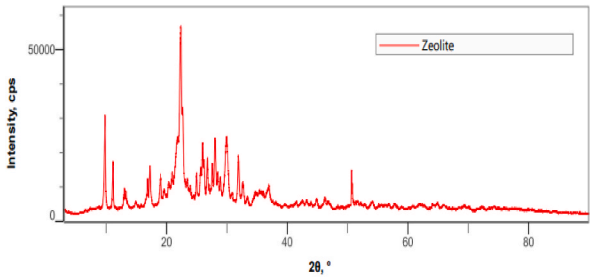

Fig. 1. X-ray diffraction patterns obtained for the HEU zeolite.

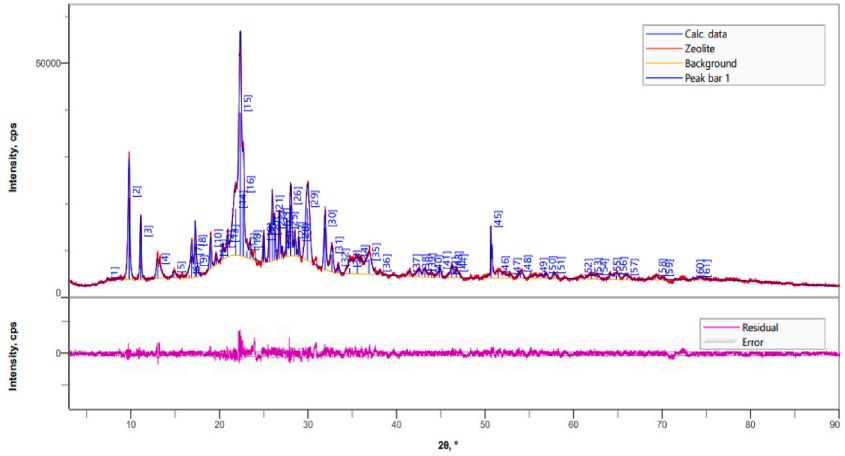

Fig. 2. Powder X-ray diffraction peak profile for the HEU zeolite.

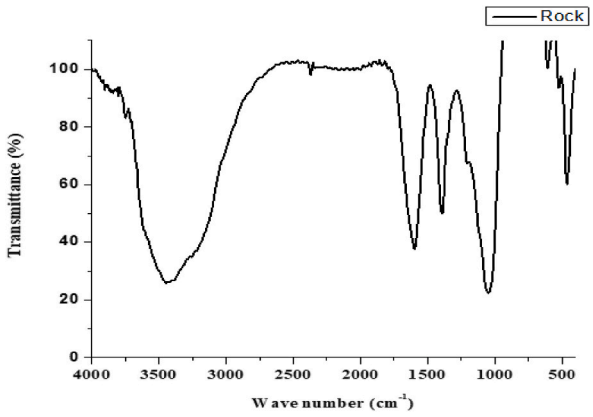

Fig. 3. FTIR spectrum of the HEU zeolite.

was analyzed in $4° \leq 2\theta \leq 70°$.

The zeolite showed distinct peaks at $2\theta = 9.8$, 11.1, 13, 22.3, 22.6, 25.9 and 30°. The peaks observed at $2\theta = 22.3°$ and 9.8° corresponds non-amorphous SiO_2 and Al_2O_3, respectively. The results from XRD reveal that the HEU zeolite was crystalline given the symmetric peaks that were sharp and of high intensity. Due to the high crystalline behavior of the HEU, its active sites can easily attract the higher initial concentration of Pb^{2+} and Cd^{2+} ions. From Fig. 2 it was observed that most of the observed peaks are highly intensive and sharp; an indication that the zeolite is highly crystalline and porous and therefore stable for adsorption studies.

FTIR spectroscopy is important in providing information on functional groups' surface identification of natural zeolites which affects the pollutants' adsorption process on adsorbent surfaces. The FTIR spectrum obtained for the HEU zeolite is shown in Fig. 3. The broad band at 3000-3600 cm^{-1} is attributed to the stretching vibration of hydroxyl groups on the surface of the zeolite and adsorbed water molecules, which possess the bending vibration mode at 1637 cm^{-1} [45]. The strong absorption band at 1036 cm^{-1} is

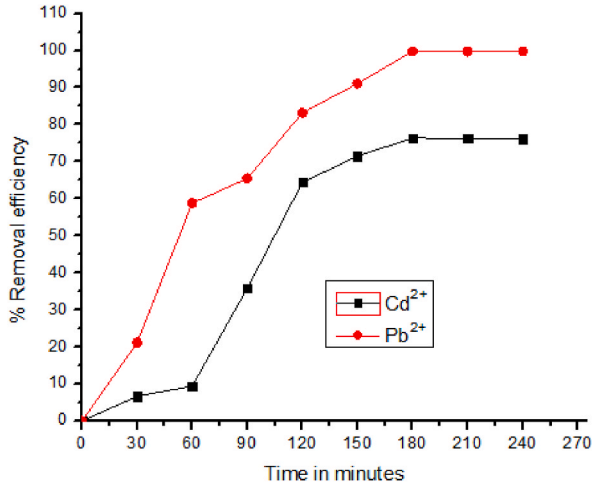

Fig. 4. Effect of contact time on the adsorption of Pb^{2+} and Cd^{2+} onto the HEU zeolite.

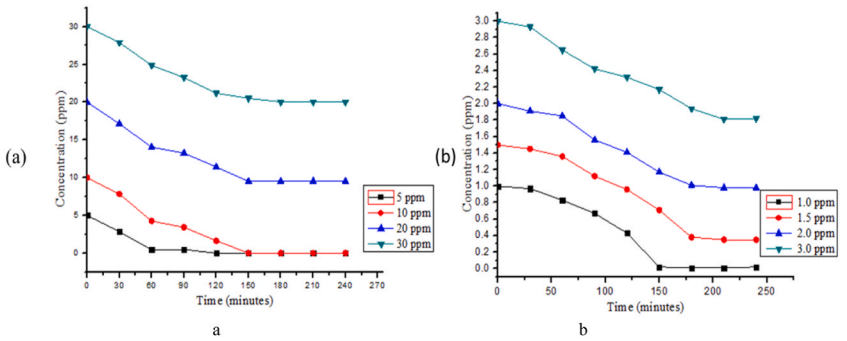

Fig. 5. Residual concentration of (a) Pb^{2+} and (b) Cd^{2+} at different initial concentrations.

attributable to silicate bond (Si–*O*–Si) while the bands at 540 and 1000 cm^{-1} are due bending vibration for Al–Al–O. Furthermore, the most intensive vibration frequency is between 1100 and 1020 cm^{-1}. This is attributable to the Si–*O*–Al structural units of the HEU zeolite [46].

3.2. Adsorption studies

3.2.1. Experimental findings

The effect of several physical factors on the adsorption behaviours of the two metal ions onto the HEU zeolite was examined. Fig. 4 shows the removal efficiency of Pb^{2+} and Cd^{2+} by the zeolite as a function of contact time (0–4 h). The zeolite's maximum adsorption capacity was reached after 3 h. Equally, from the results there was a sharp and rapid adsorption of the Pb^{2+} onto the adsorbent in the first 60 min.

On the other hand, adsorption of Cd^{2+} was slow in the first 60 min. However, the adsorption rate increases rapidly between 60 and 120 min. In both cases, the adsorption rates gradually slowed down reaching an equilibrium after 180 min. This implies that 180 min was sufficient time to attaining equilibrium. The adsorption behavior of the two metal ions can be explained by the fact that there were more active sites and a larger surface area for adsorption at the start of the experiment, which sped up mass transfer. The subsequent slow adsorption is due to the decrease in driving force caused by a decrease in active sites, up until maximum capacity is attained. The percent adsorption increased gradually as the contact time was extended to 4 h, recording 99.7 % and 76.7 % for Pb^{2+} and Cd^{2+}, respectively. The higher removal rate of Pb^{2+} compared to Cd^{2+} is due to its higher electronegativity (2.33) compared to that of Cd^{2+} (1.69) hence readily adsorbed onto the HEU zeolite. This is because a high electronegativity is responsible for the strong covalent formation between the metal ion and oxygen atoms on the zeolite surfaces [47]. From characterization, the presence of SiO_2 and Al_2O_3 indicate that the zeolite has excess negative ions that bind the heavy metal ions using cation exchange mechanisms. These results compares favorably with published results whereby most zeolites have a higher cation exchange capacity for Pb^{2+} than Cd^{2+} [48]. To study the effect of initial metal ion concentration on the adsorption of the metal ions onto HEU zeolite was investigated by varying Pb^{2+} and Cd^{2+} initial concentrations from 5 to 30 ppm and 1–3 ppm, respectively. The results obtained are show in Fig. 5a, b.

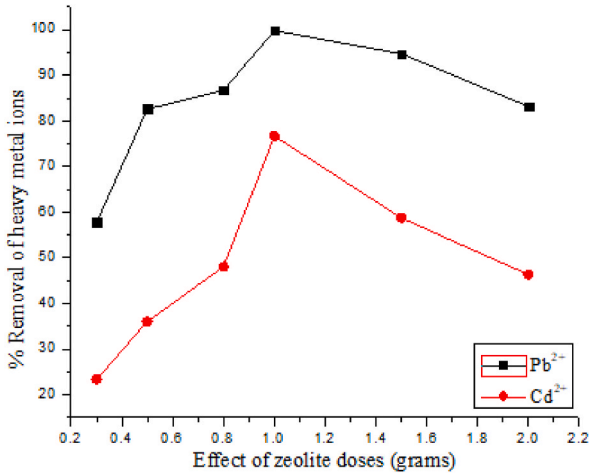

Fig. 6. Percent removal of Pb^{2+} and Cd^{2+} at different zeolite doses.

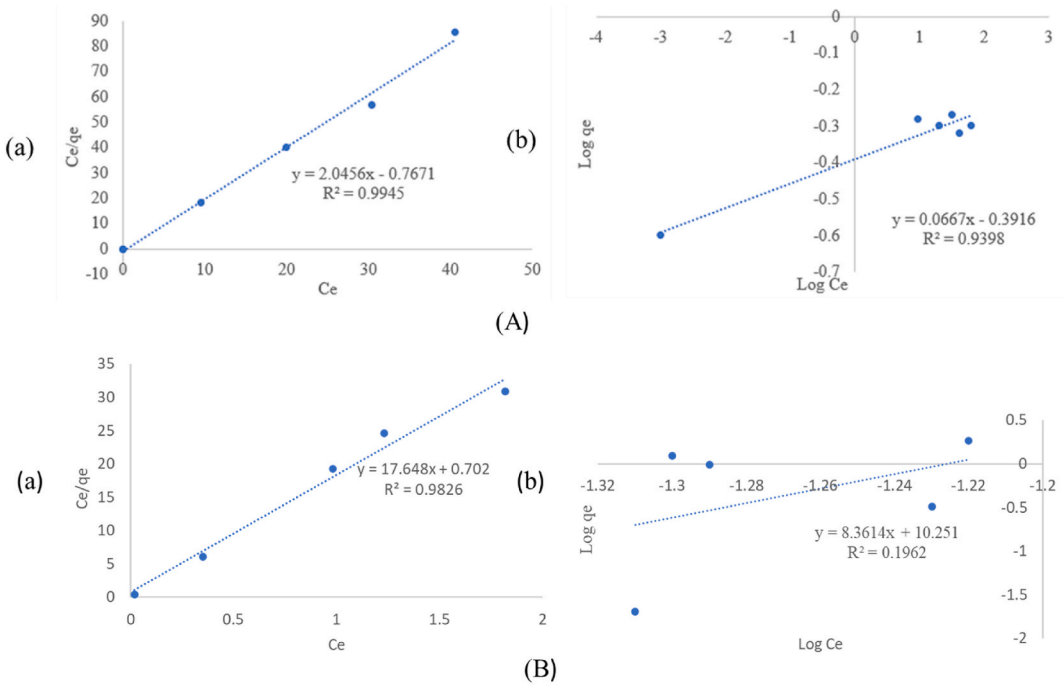

Fig. 7. Linearized (a) Langmuir and (b) Freundlich isotherms for (A) Pb^{2+} and (B) Cd^{2+} ions adsorption by zeolite.

It is worth to note that the 5 ppm Pb^{2+} concentration attained equilibrium after 60 min, while the 10 ppm concentration reached equilibrium after 150 min Fig. 5 (a). It was observed that less amounts of the adsorbate adsorb at higher initial concentrations of heavy metal ions. This is so because by increasing the number of metal ions increases the competition for the limited binding sites on the surface of the adsorbent, thereby resulting in a decreased adsorption capacity because the active sites become saturated [49].

On the case of Cd^{2+}, the adsorption followed the same trend as Pb^{2+} with the lower concentrations reaching equilibrium faster that the higher concentrations Fig. 5 (b). The adsorption values were found to be acceptable for a concentration of 10 ppm of Pb^{2+} and a concentration of 1.5 ppm of Cd^{2+}. These concentrations were chosen as the optimum values for metal ions removal. By varying the zeolite dose from 0.3 to 2.0 g at initial concentrations of 10 and 1.5 ppm of Pb^{2+} and Cd^{2+} ions, respectively, it was possible to determine the impact of adsorbent dosage on the removal of Pb^{2+} and Cd^{2+} from water. The percent removal of Pb^{2+} and Cd^{2+} ions from water at different zeolite quantities is depicted in Fig. 6.

An increase in the amount of zeolite used increases the percent removal of Pb^{2+} and Cd^{2+}ions up to a maximum amount of 1.0 g. This is attributable to increased adsorption sites as the adsorbent mass increases. Our findings are comparable with previous reports for the adsorption of Cd^{2+} and Pb^{2+} ions [50,51]. Further increase in the amount of HEU zeolite (>1.0 g) a decrease in the adsorption was

Table 2
Langmuir and Freundlich isotherms data for the adsorption of Pb^{2+} and Cd^{2+} onto HEU zeolite.

Langmuir Isotherm						
Ion	Intercept	Slope	q_{max} (mg/g)	K_L (L/mg)	R_L	R [2]
Pb^{2+}	−0.767	2.046	1.304	0.375	0.242	0.9945
Cd^{2+}	0.702	17.648	1.425	0.039	2.398	0.9826
Freundlich Isotherm						
	K_F (mg/g)		**n (L/mg)**		**R [2]**	
Pb^{2+}	−0.392		14.990		0.9398	
Cd^{2+}	10.251		0.119		0.1962	

Table 3
Previous reports on adsorption of Pb^{2+} and Cd^{2+}onto different zeolites.

Type of zeolite	Pb^{2+}		Cd^{2+}		Reference
	Adsorption capacity (mg/g)	Percent weight removal (%)	Adsorption capacity (mg/g)	Percent weight removal (%)	
Greek Natural zeolite	1.4	–	1.2	–	[54]
Bulgaria Clinoptilolite	1.6	57.0	2.4	22	[55]
Synthetic zeolite SZM-5	30.6	74.1	24.4	60.2	[56]
Ukraine Clinoptilolite	13.0		4.2	–	[57]
Turkey Clinoptilolite	27.7	92.0	–	–	[58]
Iranian Natural zeolite	52.6	–	29.4	–	[59]
Iranian sepiolite zeolite	50.0	–	19.2	–	[59]
Bulgaria Clinoptilolite	1.6	57.0	2.4	22	[60,61]
Na-A zeolite	224.7	–	118.3		[50]
Iranian Modified clinoptilolite zeolite	91.3	–	78.3	–	[62]
South African Haundatite	0.5	99.7	0.29	76.7 %	This study (Experimental)
Activated biocarbon	2.9	95	2.8	98	[63]
p-type zeolite	3.9	100	–	–	[64]
Cow manure	102.77	–	38.11	–	[65]
Extracellular polymeric substance (EPS)	31.55	94.67	23.42	94.41	[66]
Carbon nanotubes	23.4	96.7	10.5	96.7	[67]
Zr-MOFs	194.9	97	176	88	[68]
GOF	6.06	–	12.48	–	[69]
Biochar coffee	11.4	84.1	1.2	–	[70]
Activated carbon	4.1	–	7.8	–	[71]
PVC	1.3	–	0.1	–	[72]
Polystyrene particles	0.07–0.23	22.41	0.03–0.12	12.09	[73]
Iron phosphate-modified pollen microspheres as adsorbents	6.13	99	4.62	45	[74]
Turkish illitic clay	53.76	97	13.09	72	[75]

observed. This can be due to the aggregation or overlapping of zeolite particles thus reducing the adsorbent's specific surface area and the available binding sites [52]. In order to determine the uptake capacity of Pb^{2+} and Cd^{2+}ions on the HEU zeolite, Langmuir and Freundlich isothermal models were employed (Fig. 7A and B, respectively.

The Langmuir and Freundlich isothermal parameters and coefficients obtained for the adsorption of the two metal ions onto the HEU zeolite are collected in Table 2.

From the linear regression coefficient of determination (R^2) values obtained, the adsorption of Pb^{2+} and Cd^{2+} fits best in the Langmuir isotherms. This means that the adsorption of the two metal ions onto zeolite forms a mono-layer on the surface of the adsorbent with finite number of identical binding sites. This was also observed for the removal of heavy metals by other natural zeolites, hence suggesting that the mechanism may be related to its distinctive porous structure, which contains a significant number of channels and ion exchange characteristics [51,53]. Table 3 compares our results with results obtained in previous studies on the adsorption of Pb^{2+} and Cd^{2+}onto different zeolites. HEU zeolite is significantly higher than Iron phosphate-modified pollen microspheres as adsorbents for Pb^{2+} and Cd^{2+}. The results obtained in the current study are comparable with those reported in other studies. Accordingly, it could be considered a promising material for the removal of Pb^{2+} and Cd^{2+} from water.

3.2.2. Computational insights

Adsorption isotherm describes the number of ions adsorbed per cell onto the adsorbent as a function of the fluid's contact pressure at a specific temperature. This amount may vary due to temperature and initial conditions of adsorbent. Adsorption of Pb^{2+} ions onto the HEU zeolite was observed to follow a H-shaped isotherm, which is in equilibrium for Pb^{2+} with an almost maximum loading of 8 ions per unit cell. The maximum loading corresponds to a Pb^{2+} capacity of 43.36 % Fig. 8 A. The H-type isotherm indicates a gradual

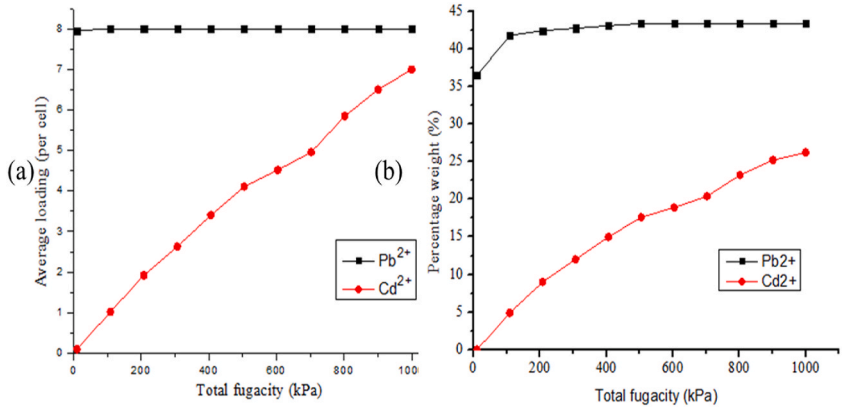

Fig. 8. Adsorption isotherms for $Pb^{2+}$and Cd^{2+} ions where (a) loading capacity and (b) percentage weight.

Table 4
The loading per cell of undoped and doped HEU zeolite.

Heavy metals	Undoped HEU	HEU doped with Germanium	HEU doped with Aluminum	HEU doped with Thallium	HEU doped with Indium	HEU doped with Sodium
Cd^{2+}	8.0	8.0	8.0	8.13	8.0	8.35
Pb^{2+}	7.0	7.48	8.46	9.34	9.12	3.53

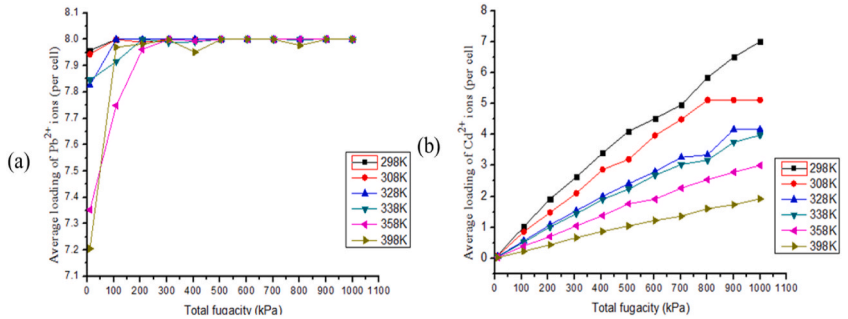

Fig. 9. Average loading of (a) Pb^{2+} and (b) Cd^{2+} ions onto HEU zeolite as a function of pressure at different temperatures.

adsorbent saturation, implying that even at low adsorbent concentrations, the Pb^{2+} ions have a considerable affinity for the adsorbent's surface [76,77]. Cd^{2+} ions, on the other hand, showed a C-shaped adsorption pattern, with a loading of 7 ions per unit cell. The weight percent capacity for Cd^{2+} ions achieved was relatively low (26.60 %) compared to that of Pb^{2+} (43.36 %). This is attributed to the fact that the zeolite was not saturated with ions and that adsorption process had not reached equilibrium. This suggests that there were still available sites within the HEU structure that could accommodate more Cd^{2+} ions, as shown in Fig. 8B.

The higher loading of Pb^{2+} than Cd^{2+} ions onto to HEU zeolite is because Pb^{2+} ions has a higher electronegativity and therefore can form strong covalent with the oxygen atoms on the HEU zeolite surfaces [47]. However, it is noted that both metal ions reached a maximum weight capacity of less than 50 %. This limitation in adsorption capacity is attributed to the small interlinked or unintercalated pores present in the HEU material. These small pores restrict the trapping of a larger number of heavy metal ions within the HEU structure, resulting in lower weight capacities for both Cd^{2+} and Pb^{2+}. The percent weight capacity, in Equation (5), was used to calculate the weight percent of the heavy metal ions adsorbed onto the HEU zeolite.

$$Percentage\ weight = \frac{Mass\ of\ the\ adsorbed\ heavy\ metal}{Mass\ of\ the\ zeolite\ used + mass\ of\ adsorbed\ lead\ (ii)\ ion} \times 100\% \quad (5)$$

The adsorption data from the Monte Carlo simulations fitted well to the Freundlich adsorption model, as depicted in Fig. 8 which shows the variation in the average loading of ions per unit mass on HEU zeolite at 298 K.

The effect of doping HEU zeolite with various elements on its loading capacity for two heavy metals ions was investigated. Specifically, the silicon atoms within the HEU structure unit cell were individually replaced by Germanium, Aluminum, Thallium, Indium, and Sodium atoms to create the doped HEU zeolite structures, which were then optimized. Table 4 displays loading of both undoped and doped HEU structure per cell.

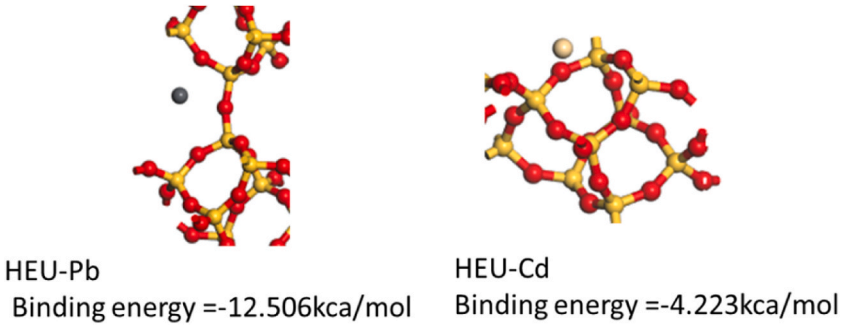

Fig. 10. The most stable structure of Pb^{2+} and Cd^{2+} adsorbed onto the HEU zeolite.

Table 5
The Pb-HEU and Cd-HEU complexes second order perturbation energy at the ώB97XDdef2svp level.

Donor NBO (i)	Acceptor NBO (j)	E [2] Kcal/mol	E(j) – E(i) a.u	F(i,j) a.u.
Pb-HEU complex				
σ*Si3–O16	σ*O1–Si3	10.11	0.02	0.060
LP (3) O1	LP (1) Al2	30.30	0.74	0.191
LP (3) O1	LP*(2) Al2	15.09	0.68	0.127
LP (3) O5	LP(4) Al10	19.50	0.82	0.161
LP (2) O13	LP* Al2	13.20	0.51	0.107
Cd-HEU complex				
LP (3) O1	LP*(1) Al2	36.99	0.80	0.220
LP (3) O1	LP*(3) Al2	18.54	0.88	0.162
LP(3) O4	LP*(1) Al2	34.28	0.84	0.217
LP(3) O4	LP*(3) Al2	24.99	0.92	0.192

Its worthy to note that when HEU is doped with Germanium, Aluminium, Indium, Thallium and Sodium the loading of Cd^{2+} ions increased compared to undoped HEU zeolite structure. The loading capacity of Pb^{2+} increased from 7 ions per cell for the undoped HEU to 7.48, 8.46, 9.12, and 9.34 ions per cell for HEU doped. In the case of Cd^{2+} only HEU doped with Thallium and Sodium showed an increase in loading. Generally, doping of HEU zeolite can effectively enhance the loading capacity of these two divalent metal ions. The adsorption isotherms of Pb^{2+} and Cd^{2+} ions at different temperatures and pressures were studied at pressures ranging from 10 to 1000 kPa and temperatures ranging from 298 to 398 K, as shown in Fig. 9.

From the results obtained, the adsorption of Pb^{2+} ions exhibit no significant effect with temperature increase. The loading of Pb^{2+} per cell remains constant at 8 ions per cell across all the temperatures studied Fig. 9 (a). On the other hand, the adsorption of Cd^{2+} per cell onto the HEU zeolite reduced as the temperature was increased. This can be due to the breaking of hydrogen bonds between the adsorbent and the Cd^{2+} ions at higher temperatures. Therefore, the loading of Cd^{2+} ions per cell decreases, with values of 7, 5, 4, 4, 3, and 2 ions per cell observed at temperatures of 298, 308, 328, 338, 358, and 398 K, respectively Fig. 9 (b). The adsorption difference of Pb^{2+} and Cd^{2+} ions regarding temperature dependence is due to differences in the nature of the interactions between the HEU zeolite and the metal ions. Fig. 10 displays the most stable structural configurations of Pb^{2+} and Cd^{2+} adsorbed onto the HEU zeolite.

In the case of Pb^{2+}, the ions are adsorbed at the window of the HEU zeolite, equidistant from two adjacent oxygen atoms on the structure. This suggests that Pb^{2+} ions form stable bonds with the oxygen atoms in the zeolite framework. In contrast, Cd^{2+} ions are adsorbed on upper left side of the 8-ring HEU window. The adsorption energy for Pb^{2+} and Cd^{2+}ions on the HEU zeolite structure were −12.51 and −4.22 kcal/mol, respectively. The adsorption process is exothermic as indicated by the negative energy. Based on the binding energy results, it can be inferred that Pb^{2+} sorption onto the HEU zeolite is preferable to Cd^{2+} sorption. The higher adsorption energy observed for Pb^{2+} suggests stronger interactions between the Pb^{2+} ions and the zeolite structure framework, indicating a more stable adsorption configuration for Pb^{2+} on the HEU structure. Information on charge density transfer and molecular stabilization due to electronic delocalization is a key aspect that provides valuable insights into chemical bonding and reactivity. This allows for the evaluation of the extent to which electronic delocalization or charge density transfer contributes to molecular stabilization. Natural bond orbitals are a useful tool in scrutinizing the chemical characteristics of a given compound. It can provide information on the basicity, stability, intra- and intermolecular charge transfer. In addition, it provides information on the link between donor and acceptor molecular orbitals [78]. In this study we conducted NBO analyses to gain insights on the charge delocalization and molecular stabilization in Pb-HEU and Cd-HEU complexes. The second-order perturbation energies and the various sites of contribution from different excitation types for the Pb-HEU and Cd-HEU complexes were analyzed and are recorded in Table 5.

The total stabilization interaction for charge transfer was reported with respect to Mohammadi and coworkers [79]. The results have shown that the stabilization energies of the Pb-HEU complex ranged between 10.11 and 30.30 kcal/mol, with the σ→ σ interaction having the lowest $E^{(2)}$ contribution of 10.11 kcal/mol. The Cd-HEU complex had higher stabilization energies ranging from 18.54 to 36.99 kcal/mol, with the LP→LP* molecular orbital contributing the highest stabilization energy of 147.47 kcal/mol. The

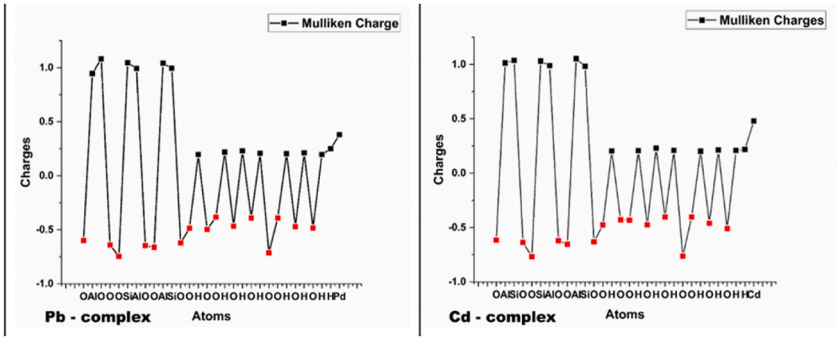

Fig. 11. Mulliken population charge analysis of the Pb-HEU and Cd-HEU complexes.

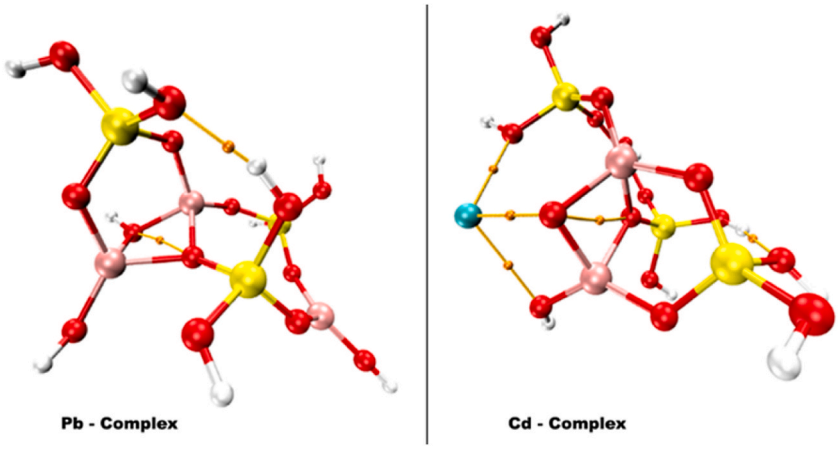

Fig. 12. The critical point (C.P.) between each intramolecular interaction in the Pb-HEU and Cd-HEU complexes.

high stabilization energy values demonstrate the system's stability as a result of a robust donor-to-acceptor intermolecular connection. As a result, the Cd-HEU complex system with the highest $E^{(2)}$ value is the most stable. The total change in charge density transfer for the Pb-HEU complex was 49.80 kcal/mol for ΔETLP → L.P. and 28.29 kcal/mol for ΔETLP → L.P*., which contributed to the stability of the Pb-HEU complex. In contrast, the Cd-HEU complex was stabilized by the LP→LP molecular orbital interaction.

The delocalization of charge density in molecules is an important factor in predicting a system's conformational characteristics and reactivity. Delocalization and Mulliken charge analysis play a crucial role in charge transformative processes, electronegativity equalization, and the potential energy surface [80,81]. Mulliken charge analysis is calculated at the ωBb97XD/def2svp theoretical level to analyse the charge density distribution and delocalization over the whole complex. This analysis can help in understanding how the electron density is distributed and transferred during chemical reactions, as well as in identifying the most reactive sites in a molecule. Fig. 11 shows Mulliken population charge analysis of the Pb-HEU and Cd-HEU complexes. It was observed that in the two complexes have higher negative densities due to the presence of negatively charged oxygen between the two hydroxyl groups (OH–*O*–OH) and linked to silicon atom (Si–O). This clearly shows that these immensely negatively charge oxygen atoms attract a higher electronic distribution than other charged atoms in the complexes.

Remarkably, the presence of positively charged aluminum (AI) in both complexes resulted in a shift in the electronic charge delocalization, with the Pb-HEU complex shifting from −0.80 to 1.55 eV and the Cd-HEU complex shifting from 0.7 to 1.30 eV.

The Quantum Theory of Atoms in Molecules (QTAIM) which is a theoretical framework was utilized extensively to better understand the behavior of inter- or intramolecular hydrogen bonding interaction at molecular and atomic levels using electronic charge density. Also, QTAIM provides insights into chemical reactivity and molecular recognition. The QTAIM theory partitions a molecule into atoms using its electronic charge density, which could be obtained computationally or experimentally. Various critical points are identified by evaluating the first and second derivatives of the electron density, which are used to characterize a number of non-covalent interactions such as intermolecular hydrogen bonding within atoms in the molecule. QTAIM can also be used to identify and characterize molecules which possess non-covalent bonds. Therefore, information on the electron density at different bond critical points (bcps) of an intra- or intermolecular hydrogen bond interaction can be utilized to determine the strength of the hydrogen bond. Hence, the concept of QTAIM formulated by Bader and coworkers [82], was used to study Pb-HEU and Cd-HEU complexes to characterize the features of the intermolecular hydrogen bonds present. Fig. 12 illustrates the critical point (C.P.) between each intramolecular interaction, providing insights into the strength of hydrogen bonding within Pb-HEU and Cd-HEU complexes.

Table 6
QTAIM parameters for Pb-HEU and Cd-HEU complex systems.

Systems	Parameters	Bond	p(r)	∇ [2] p(r)	G(r)	K(r)	V(r)	H(r)	G(r)/V(r)	ELF	Ɛ	λ_1	λ_2	λ_3
Pb-HEU complex	BCPs	O_5–O_{15}	0.85	0.76	0.18	−0.52	−0.17	−0.52	−1.06	0.61	0.04	−0.15	−0.16	0.10
	BE($E_{O—O}$)	−188.88												
	BCPs	O_{18}–H_{26}	0.11	0.91	0.24	0.13	−0.25	−0.13	−0.96	0.91	0.01	0.13	−0.20	−0.21
	BE($E_{O—H}$)	−23.79												
Cd-HEU complex	BCPs	O_{22}–Cd_{30}	0.67	0.36	0.98	0.72	−0.10	−0.72	−9.80	0.94	0.01	0.52	−0.77	−0.78
	BE($E_{O—Cd}$)	−148.72												
	BCPs	Cd_{30}–O_{27}	0.33	0.14	0.36	0.14	−0.36	−0.14	−1.00	0.73	0.05	0.20	−0.32	−0.31
	BE($E_{Cd—O}$)	−72.87												
	BCPs	Cd_{30}–O_{18}	0.24	0.92	0.22	−0.60	−0.21	0.60	−1.05	0.65	0.05	0.13	−0.19	−0.20
	BE($E_{Cd—O}$)	−52.79												
	BCPs	O_{22}–O_{22}	0.32	0.14	0.33	−0.19	−0.31	0.19	−1.06	0.77	5.28	−0.28	0.17	−0.45
	BE($E_{O—O}$)	−70.64												
	BCPs	O_{25}–H_{29}	0.35	0.13	0.33	−0.55	−0.32	0.55	−1.03	0.10	0.03	0.26	−0.63	−0.61
	BE($E_{O—H}$)	−77.33												

Table 6 provides additional information on the nature and strength of the bonding interactions within the studied Pb-HEU and Cd-HEU complexes. The Laplacian of electron density (2BCP), ellipticity, potential energy density V(r), kinetic energy density G(r), total energy H(r), binding energy at the critical points, and the G(r)/V(r) ratio are all given in Table 6. The binding energy at the bond critical points (BCPs) [EO5-O15, EO22-H26] for the Pb-HEU and Cd-HEU complexes was −188.88 and −23.79 kcal/mol, respectively. It is worth noting that no bond critical point of interaction between Pb and other atoms was detected, indicating weak or no interaction. In contrast, a significant chemisorption interaction was observed for O_{22}–Cd_{30} and Cd_{30}–O_{27} bond critical points, with a binding energy (B.E.) of −148.72 and −72.87 kcal/mol respectively. This suggests a strong interaction between Cd and the oxygen atoms, which can have significant implications for the properties and behavior of the complex. The higher binding energy observed for the Cd and O interaction indicates stronger stability of Cd-HEU complexes, which is the complex's second-order perturbation energy $E^{(2)}$. This is because BE is directly proportional to stability of a complex [78]. The positive Laplacian electron density observed in Pb-HEU and Cd-HEU complexes show that the most prominent interactions in the two complexes is electrostatic in nature (Table 6). The concept of ellipticity (Ɛ), which is calculated using the negative Hessian of the electron density at Bond Critical Points (BCPs), is expressed as $\mathcal{E} = \lambda_1/\lambda_2 - 1$, where λ_1 and λ_2 represent the eigenvalues of the negative Hessian of electron density at BCPs. As a result, the parallel expansion λ_1/λ_2 and ellipticity values for the Pb-HEU complex and Cd-HEU complex systems are less than one, indicating a highly strong intermolecular interaction between the HEU zeolite and the heavy metal ions. Therefore, the adsorption interactions studied were highly plausible. The investigated compounds have high stability, with the Cd-HEU combination having the most stable chemisorption bonds with an oxygen atom at the aromatic ring.

4. Conclusions

In this study the removal of Pb^{2+} and Cd^{2+} from water by adsorption by HEU zeolite was investigated through batch experiments and theoretical simulations. The zeolite was characterized using EDX, XRD, and FTIR techniques. The results indicate that the HEU zeolite effectively removed Pb^{2+} and Cd^{2+} ions from water. The equilibrium studies demonstrated that HEU zeolite had a higher affinity for Pb^{2+} ions compared to Cd^{2+} ions, and the adsorption process occurred rapidly. Factors such as zeolitic pore size, metal ion size and electronegativity, and hydration all influenced the zeolite's capacity to adsorb the metal ions. The experimental and computational studies revealed that the percent weight capacity of the zeolite for the two ions followed the decreasing order of $Pb^{2+} > Cd^{2+}$. This trend suggests that the zeolite had a higher adsorption capacity for Pb^{2+} ions compared to Cd^{2+}. Furthermore, the BE at the BCPs for the Pb-HEU complex was −188.88 kcal/mol and −148.72 kcal/mol for the Cd-HUE complex. The stronger binding energy of the interaction between Pb and HEU provides a rationale for Pb's greater percent weight capacity on the zeolite compared to Cd, as shown by the experimental results. The results suggest that different excitation types contribute differently to the stabilization energy and charge transfer in these complexes, with the Cd-HEU complex showing a higher degree of stabilization than the Pb-HEU complex. These findings could have implications for understanding the properties and behavior of these complexes in environmental remediation. This study shows that the doped or modified HEU zeolite shows high sorption ability toward all cations studied. This suggests that the modified zeolite has the potential to effectively adsorb different cations. Meanwhile, being locally available, and freely abundant with a considerably high adsorption capacity, natural zeolite is an attractive choice for removing metal ions from wastewater.

Data availability statement

All data are contained within the manuscript and electronic supporting information (ESI)

CRediT authorship contribution statement

Fred S. Wanyonyi: Project administration. **Francis Orata:** Formal analysis. **Gershom K. Mutua:** Investigation. **Michael O. Odey:** Investigation. **Sizwe Zamisa:** Methodology. **Sopuruchukwu E. Ogbodo:** Formal analysis. **Francis Maingi:** Data curation. **Anthony Pembere:** Resources.

Declaration of competing interest

The authors declare that they have no known competing financial interests or personal relationships that could have appeared to influence the work reported in this paper.

Acknowledgements

We acknowledge the support by Masinde Muliro University of Science and Technology, Kenya, University of Kwazulu Natal, South Africa, University of Johannesburg, South Africa and Center for High Performance Computing, South Africa.

Appendix A. Supplementary data

Supplementary data to this article can be found online at https://doi.org/10.1016/j.heliyon.2024.e34657.

References

[1] F. Elbehiry, H. Elbasiouny, R. Ali, E.C. Brevik, Enhanced immobilization and phytoremediation of heavy metals in landfill contaminated soils, Water, Air, Soil Pollut. 231 (2020) 1–20.
[2] L. Ren, J. Xu, Y. Zhang, J. Zhou, D. Chen, Z. Chang, Preparation and characterization of porous chitosan microspheres and adsorption performance for hexavalent chromium, Int. J. Biol. Macromol. 135 (2019) 898–906.
[3] S. Pandey, A comprehensive review on recent developments in bentonite-based materials used as adsorbents for wastewater treatment, Jorunal Of Molecular Liqiuds vol. 241 (2017) 1091–1113.
[4] M. Buaisha, S. Balku, S. Özalp-Yaman, Heavy metal removal investigation in conventional activated sludge systems, Civil Engineering Journal 6 (2020) 470–477.
[5] F. Orata, Chemicals of emerging concern in surface and wastewater: a perspective of their fate within the lake victoria catchment area of Kenya, in: Effects of Emerging Chemical Contaminants on Water Resources and Environmental Health, IGI Global, 2020, pp. 1–16.
[6] A.A. Tinkov, T. Filippini, O.P. Ajsuvakova, M.G. Skalnaya, J. Aaseth, G. Bjørklund, E.R. Gatiatulina, E.V. Popova, O.N. Nemereshina, P.-T.J. E. r. Huang, Cadmium and atherosclerosis: a review of toxicological mechanisms and a meta-analysis of epidemiologic studies 162 (2018) 240–260.
[7] W. Lin, L. Jing, B. Zhang, Micellar-enhanced ultrafiltration to remove nickel ions: a response surface method and artificial neural network optimization, Water 12 (2020) 1269.
[8] M. Kumar, L. Goswami, A.K. Singh, M. Sikandar, Valorization of coal fired-fly ash for potential heavy metal removal from the single and multi-contaminated system, Heliyon 5 (2019) e02562.
[9] S. Bolisetty, M. Peydayesh, R. Mezzenga, Sustainable technologies for water purification from heavy metals: review and analysis, Chem. Soc. Rev. 48 (2019) 463–487.
[10] G. Zhao, X. Wu, X. Tan, X. Wang, Sorption of heavy metal ions from aqueous solutions: a review, Open Colloid Sci. J. 4 (2010).
[11] Y. Zhang, X. Duan, Chemical precipitation of heavy metals from wastewater by using the synthetical magnesium hydroxy carbonate, Water Sci. Technol. 81 (2020) 1130–1136.
[12] A. Pohl, Removal of heavy metal ions from water and wastewaters by sulfur-containing precipitation agents, Water, Air, Soil Pollut. 231 (2020) 1–17.
[13] Y. Sun, S. Zhou, P.-C. Chiang, K.J. Shah, Evaluation and optimization of enhanced coagulation process: water and energy nexus, Water-Energy Nexus 2 (2019) 25–36.
[14] R. Kejriwal, M. Mandke, P. Ingle, Bio-sorption of heavy metals: a review, International Journal of Advanced Research in Chemical Science (IJARCS (2018) 32–42.
[15] P. Kehrein, M. Van Loosdrecht, P. Osseweijer, M. Garfí, J. Dewulf, J. Posada, A critical review of resource recovery from municipal wastewater treatment plants–market supply potentials, technologies and bottlenecks, Environ. Sci. J. Integr. Environ. Res.: Water Research & Technology 6 (2020) 877–910.
[16] P.P. Mashile, A. Mpupa, P.N. Nomngongo, Adsorptive removal of microcystin-Lr from surface and wastewater using tyre-based powdered activated carbon: kinetics and isotherms, Toxicon 145 (2018) 25–31.
[17] I. Ali, New generation adsorbents for water treatment, Chem. Rev. 112 (2012) 5073–5091.
[18] M. Moazeni, S. Parastar, M. Mahdavi, A. Ebrahimi, Evaluation efficiency of Iranian natural zeolites and synthetic resin to removal of lead ions from aqueous solutions, Appl. Water Sci. 10 (2020) 1–9.
[19] R. Sharma, P.R. Agrawal, R. Kumar, G.J. C.o.W. Gupta, Current Scenario of Heavy Metal Contamination in Water, 2021, pp. 49–64.
[20] B.R.S. De Araujo, J.A. Onrubia-Calvo, I. Stambouli, G. Pétaud, J. Hidalgo-Carrillo, A. Nieto-Marquéz, B. Pereda-Ayo, J.R. González-Velasco, A. Caravaca, S. Gil, Towards the development of advanced hierarchical chabazite materials: novel micro-mesoporous silicoaluminophosphate sapo-34 zeolites, Mater. Today Commun. (2022) 103580.
[21] I. Marantos, G.E. Christidis, M. Ulmanu, Zeolite Formation and deposits, Handbook of natural zeolites (2012) 28–51.
[22] E. Ugwu, A. Othmani, C. Nnaji, Technology, A Review on Zeolites as Cost-Effective Adsorbents for Removal of Heavy Metals from Aqueous Environment, Int.J. Environ.Sci.Tech 19 (2022) 8061–8084.
[23] M. Hong, L. Yu, Y. Wang, J. Zhang, Z. Chen, L. Dong, Q. Zan, R. Li, Heavy metal adsorption with zeolites: the role of hierarchical pore architecture, Chem. Eng. J. 359 (2019) 363–372.
[24] S.E. Lehman, S.C. Larsen, Zeolite and mesoporous silica nanomaterials: greener syntheses, environmental applications and biological toxicity, Environ. Sci.: Nano 1 (2014) 200–213.
[25] K. Wang, B. Jia, Y. Li, J. Sun, X. Wu, Explorations on thermodynamic and kinetic performances of various cationic exchange durations for synthetic clinoptilolite, Molecules 27 (2022) 2597.
[26] C.D. Williams, Synthesis of pure clinoptilolite without the use of seed crystals, Chem. Commun. (1997) 2113–2114.
[27] D.S. Coombs, A. Alberti, T. Armbruster, G. Artioli, C. Colella, E. Galli, J.D. Grice, F. Liebau, J.A. Mandarino, H. Minato, Recommended nomenclature for zeolite minerals; report of the subcommittee on zeolites of the international mineralogical association, commission on new minerals and mineral names, Can. Mineral. 35 (1997) 1571–1606.
[28] N. Rajic, D. Stojakovic, M. Jovanovic, N.Z. Logar, M. Mazaj, V. Kaucic, Removal of nickel (ii) ions from aqueous solutions using the natural clinoptilolite and preparation of nano-nio on the exhausted clinoptilolite, Appl. Surf. Sci. 257 (2010) 1524–1532.
[29] K.K. Kapanji, The removal of heavy metals from wastewater using South African clinoptilolite, Cités (2009).
[30] F.S. Wanyonyi, T.T. Fidelis, H. Louis, G.K. Mutua, F. Orata, L. Rhyman, P. Ramasami, A.M. Pembere, Simulation guided prediction of zeolites for the sorption of selected anions from water: machine learning predictors for enhanced loading, J. Mol. Liq. 355 (2022) 118913.
[31] F.S. Wanyonyi, T.T. Fidelis, G.K. Mutua, F. Orata, A.M. Pembere, Role of pore chemistry and topology in the heavy metal sorption by zeolites: from molecular simulation to machine learning, Comput. Mater. Sci. 195 (2021) 110519.
[32] P.P. Diale, S. Mkhize, E. Muzenda, J. Zimba, The Sequestration of Heavy Metals Contaminating the Wonderfonteinspruit Catchment Area Using Natural Zeolite, 2011.
[33] I. Langmuir, The adsorption of gases on plane surfaces of glass, mica and platinum, J. Am. Chem. Soc. 40 (1918) 1361–1403.
[34] R. Chakraborty, R. Verma, A. Asthana, S.S. Vidya, A.K. Singh, Adsorption of hazardous chromium (vi) ions from aqueous solutions using modified sawdust: kinetics, isotherm and thermodynamic modelling, Int. J. Environ. Anal. Chem. 101 (2021) 911–928.
[35] M.M. Majd, V. Kordzadeh-Kermani, V. Ghalandari, A. Askari, M. Sillanpää, Adsorption Isotherm Models: A Comprehensive and Systematic Review (2010–2020), Sci. Total Environ. (2021) 151334.
[36] N.M. Mahmoodi, B. Hayati, M. Arami, C. Lan, Adsorption of textile dyes on pine cone from colored wastewater: kinetic, equilibrium and thermodynamic studies, Desalination 268 (2011) 117–125.
[37] D.A. Almasri, T. Rhadfi, M.A. Atieh, G. McKay, S. Ahzi, High performance hydroxyiron modified montmorillonite nanoclay adsorbent for arsenite removal, Chem. Eng. J. 335 (2018) 1–12.
[38] C. Baerlocher, L.B. McCusker, D.H. Olson, Atlas of Zeolite Framework Types, Elsevier, 2007.
[39] B. Delley, From molecules to solids with the dmol 3 approach, J. Chem. Phys. 113 (2000) 7756–7764.
[40] M. Frisch, G. Trucks, H. Schlegel, G. Scuseria, M. Robb, J. Cheeseman, G. Scalmani, V. Barone, B. Mennucci, G.J.I. Petersson, Wallingford, CT, USA, jcadj, fox Gaussian 09, revision C. 01. Gaussian, 2010.
[41] T. Lu, F.J. J.o. c. c. Chen, Multiwfn: A Multifunctional Wavefunction Analyzer, vol. 33, 2012, pp. 580–592.
[42] P. Diale, S. Mkhize, E. Muzenda, J. Zimba, The sequestration of heavy metals contaminating the wonderfonteinspruit catchment area using natural zeolite, World Academy of Science, Engineering and Technology 74 (2011) 766–772.
[43] S.M. Auerbach, K.A. Carrado, P.K. Dutta, Handbook of Zeolite Science and Technology, CRC press, 2003.
[44] S. Nair, A.H.M.S. Hussain, B.J. Tatarchuk, The role of surface acidity in adsorption of aromatic sulfur heterocycles from fuels, Fuel 105 (2013) 695–704.

[45] Isbn 0 412 53380 4. 1995, in: C.V.J.G.M. Jeans, Mj Wilson (Eds.), Clay Mineralogy: Spectroscopic and Chemical Determinative Methods, Xi+ 367, vol. 132, Chapman & Hall. Price£ 79.00 (Hard Covers), London, Glasgow, Weinheim, New York, Tokyo, Melbourne, Madras, 1994, 250-250.
[46] T. A Saleh, V. K Gupta, Characterization of the chemical bonding between Al2o3 and nanotube in mwcnt/Al2o3 nanocomposite, Curr. Nanosci. 8 (2012) 739–743.
[47] X. Zhao, F. Gu, Y. Wang, Z. Peng, J. Liu, Surface electronegativity as an activity descriptor to screen oxygen evolution reaction catalysts of Li–O2 battery, ACS Appl. Mater. Interfaces 12 (2020) 27166–27175.
[48] L. Velarde, M.S. Nabavi, E. Escalera, M.-L. Antti, F. Akhtar, Adsorption of heavy metals on natural zeolites: a review, Chemosphere (2023) 138508.
[49] H. El-Araby, A. Ahmed Ibrahim, A. Mangood, Technology, Removal of Copper (Ii) and Cadmium (Ii) Ions from Aqueous Solution by Adsorption on Modified Almond Shells, Int. J. Eng. Technol. vol. 19 (2019) 1–39.
[50] W.-w. Bao, H.-f. Zou, S.-c. Gan, X.-c. Xu, G.-j. Ji, K. Zheng, Adsorption of Heavy Metal Ions from Aqueous Solutions by Zeolite Based on Oil Shale Ash: Kinetic and Equilibrium Studies, Chem. Res. Chin. Univ. vol. 29 (2013) 126–131.
[51] M. Sayed, M.S. Khater, Removing Cadmium and Lead from Wastewater Using Natural Zeolite Isotherm Models, J. Appl. Sci. vol. 3 (2013) 98–104.
[52] T. Yousefi, M.A. Mohsen, H.R. Mahmudian, M. Torab-Mostaeidi, M.A. Moosavian, H.J. J.o.W. Aghayan, E. Nanotechnology, Removal of Pb (Ii) by Modified Natural Adsorbent; Thermodynamics and Kinetics Studies, vol. 3, 2018, pp. 265–272.
[53] I. Kithinji Kinoti, J. Ogunah, M. Muturia, C. Thiruaine, J.M. Marangu, Adsorption of heavy metals in contaminated water using zeolite derived from agro-wastes and clays, Review (2022).
[54] E. Malliou, M. Loizidou, N. Spyrellis, Uptake of lead and cadmium by clinoptilolite, Sci. Total Environ. 149 (1994) 139–144.
[55] S. Babel, T.A. Kurniawan, Low-cost adsorbents for heavy metals uptake from contaminated water: a review, J. Hazard Mater. 97 (2003) 219–243.
[56] R.R. Mukti, Characteristics of heavy metals adsorption Cu, Pb and Cd Using Synthetics Zeolite Zsm-5 20 (2016) 77–83.
[57] M. Sprynskyy, B. Buszewski, A.P. Terzyk, J. Namieśnik, Study of the selection mechanism of heavy metal (Pb2+, Cu2+, Ni2+, and Cd2+) adsorption on clinoptilolite, J. Colloid Interface Sci. 304 (2006) 21–28.
[58] M.J. J.o. h. m. Karatas, Removal of Pb (Ii) from Water by Natural Zeolitic Tuff: Kinetics and Thermodynamics, vol. 199, 2012, pp. 383–389.
[59] S. Ghahfarokhi, A. Landi, H. Khademi, S.J.J.E.S. Hojati, Removal of Cd2+ and Pb2+ Ions from Aqueous Solutions Using Iranian Natural Zeolite and Sepiolite, vol. 40, 2014, p. 43.
[60] M. Zamzow, B. Eichbaum, K. Sandgren, D. Shanks, Removal of heavy metals and other cations from wastewater using zeolites, Separ. Sci. Technol. 25 (1990) 1555–1569.
[61] S.M. Shaheen, A.S. Derbalah, F.S. Moghanm, Development, Removal of Heavy Metals from Aqueous Solution by Zeolite in Competitive Sorption System, Int. J. Environ. Sci. Dev. Monit 3 (2012) 362–367.
[62] M.R. Mirbaloochzehi, A. Rezvani, A. Samimi, M. Shayesteh, Application of a Novel Surfactant-Modified Natural Nano-Zeolite for Removal of Heavy Metals from Drinking Water, Indian J. Chem., Sect. A vol. 3 (2020) 612–620.
[63] M.J.S.A. Singanan, Removal of Lead (Ii) and Cadmium (Ii) Ions from Wastewater Using Activated Biocarbon, vol. 37, 2011, pp. 115–119.
[64] C. Mingyue, N. Shuying, Z. Yantao, S.R. Muhammad, X. Yi, M.S. Molokeev, H. Fuqiang, Renewable P-type Zeolite for Superior Absorption of Heavy Metals: Isotherms, Kinetics, and Mechanism, 2020.
[65] W. Zhu, W. Du, X. Shen, H. Zhang, Y.J.E.P. Ding, Comparative Adsorption of Pb2+ and Cd2+ by Cow Manure and its Vermicompost, vol. 227, 2017, pp. 89–97.
[66] D. Cui, C. Tan, H. Deng, X. Gu, S. Pi, T. Chen, L. Zhou, A.J.A. Li, Biosorption Mechanism of Aqueous Pb 2+, Cd 2+, and Ni 2+ Ions on Extracellular Polymeric Substances (Eps), 2020, p. 2020.
[67] M. Šolić, S. Maletić, M.K. Isakovski, J. Nikić, M. Watson, Z. Kónya, S. Rončević, Removing Low Levels of Cd (Ii) and Pb (Ii) by Adsorption on Two Types of Oxidized Multiwalled Carbon Nanotubes, J. Environ. Chem. Eng. vol. 9 (2021) 105402.
[68] S. Gul, Z. Ahmad, M. Asma, M. Ahmad, K. Rehan, M. Munir, A.A. Bazmi, H.M. Ali, Y. Mazroua, M.A.J.C. Salem, Effective Adsorption of Cadmium and Lead Using So3h-Functionalized Zr-Mofs in Aqueous Medium, vol. 307, 2022 135633.
[69] A. Shekarizadeh, R. Azadi, R.J.S.I. Mirzajani, Synthesis of a new porous graphene oxide framework (gof) for high-performance ultrasonic-assisted removal of cadmium and lead ions from aqueous solution 30 (2023) 2029–2042.
[70] R. Carnier, A.R. Coscione, C.A.d. Abreu, L.C.A. Melo, A.F.d.J.B. Silva, Cadmium and Lead Adsorption and Desorption by Coffee Waste-Derived Biochars, vol. 81, 2022 e0622.
[71] A.K. Kamau, Removal of lead (ii) and cadmium (ii) ions from wastewater using activated carbon derived from macadamia intergrifolia nutshell powder, JKUAT-COPAS (2022).
[72] F. Gao, J. Li, C. Sun, L. Zhang, F. Jiang, W. Cao, L.J. M.p. b. Zheng, Study on the capability and characteristics of heavy metals enriched on microplastics in marine, Environment 144 (2019) 61–67.
[73] B.S. Barus, K. Chen, M. Cai, R. Li, H. Chen, C. Li, J. Wang, S.-Y. Cheng, Heavy Metal Adsorption and Release on Polystyrene Particles at Various Salinities, Frontires Of Marine Science vol. 8 (2021) 671802.
[74] X. Zhang, H. Liu, J. Yang, L. Zhang, B. Cao, L. Liu, W.J. R.o. a. m. s. Gong, Removal of Cadmium and Lead from Aqueous Solutions Using Iron Phosphate-Modified Pollen Microspheres as Adsorbents, vol. 60, 2021, pp. 365–376.
[75] D. Ozdes, C. Duran, H.B. Senturk, Adsorptive Removal of Cd (Ii) and Pb (Ii) Ions from Aqueous Solutions by Using Turkish Illitic Clay, J.Environ.Manag vol. 92 (2011) 3082–3090.
[76] G. de Vargas Brião, M.G. da Silva, M.G.A. Vieira, Expanded vermiculite as an alternative adsorbent for the dysprosium recovery, J. Taiwan Inst. Chem. Eng. 127 (2021) 228–235.
[77] A. Bonilla-Petriciolet, D.I. Mendoza-Castillo, H.E. Reynel-Ávila, Adsorption Processes for Water Treatment and Purification, vol. 256, Springer, 2017.
[78] H. Louis, G.E. Mathias, O.J. Ikenyirimba, T.O. Unimuke, D. Etiese, A.S. Adeyinka, Metal-doped Al12n12x (X= Na, Mg, K) nanoclusters as nanosensors for carboplatin: insight from first-principles computation, J. Phys. Chem. B 126 (2022) 5066–5080.
[79] M.D. Mohammadi, F. Abbas, H. Louis, G.E. Mathias, T.O. Unimuke, Trapping of Co, Co2, H2s, Nh3, No, No2, and so2 by polyoxometalate compound, Computational and Theoretical Chemistry 1215 (2022) 113826.
[80] A. Hussain, M.U. Khan, M. Ibrahim, M. Khalid, A. Ali, S. Hussain, M. Saleem, N. Ahmad, S. Muhammad, A.G. Al-Sehemi, Structural parameters, electronic, linear and nonlinear optical exploration of thiopyrimidine derivatives: a comparison between dft/tddft and experimental study, J. Mol. Struct. 1201 (2020) 127183.
[81] H. Louis, G.E. Mathias, T.O. Unimuke, W. Emori, L. Ling, A.E. Owen, A.S. Adeyinka, T.N. Ntui, C.-R. Cheng, Isolation, characterization, molecular electronic structure investigation, and in-silico modeling of the anti-inflammatory potency of trihydroxystilbene, J. Mol. Struct. (2022) 133418.
[82] S. Esser, Qtaim and the interactive conception of chemical bonding, Philos. Sci. 86 (2019) 1307–1317.